

Role of potential on high-order harmonic generation from atoms irradiated by bichromatic counter-rotating circularly polarized laser fields*

Xu-Xu Shen(申许许)¹, Jun Wang(王俊)¹, Fu-Ming Guo(郭福明)¹,
Ji-Gen Chen(陈基根)², and Yun-Jun Yang(杨玉军)^{1,†}

¹Institute of Atomic and Molecular Physics, Jilin University, Changchun 130012, China

²Zhejiang Provincial Key Laboratory for Cutting Tools, Taizhou University, Taizhou 318000, China

(Received 23 February 2020; revised manuscript received 21 May 2020; accepted manuscript online 25 May 2020)

We investigate high-order harmonic generation from atoms irradiated by bichromatic counter-rotating circularly polarized laser pulses by numerically solving the time-dependent Schrödinger equation. It is found that the minimum energy position of the harmonic spectrum and the non-integer order optical radiation are greatly discrepant for different atomic potentials. By analyzing the quantum trajectory of the harmonic emission, discrepancies among the harmonic spectra from different potentials can be attributed to the action of the potential on the ionized electrons. In addition, based on the influence of the driving light intensity on the overall intensity and ellipticity of higher order harmonics, the physical conditions for generating a high-intensity circularly polarized harmonic can be obtained.

Keywords: high-order harmonic generation, bichromatic counter-rotating circularly polarized laser fields, channel closing effect, quantum trajectory interference

PACS: 32.80.Rm, 42.50.Hz

DOI: 10.1088/1674-1056/ab961c

1. Introduction

With the rapid development of the femtosecond intense laser pulse technology, amplitude of laser electric field has reached the magnitude of the electronic field for an electron acted by the nucleus. When an atom is irradiated by such an intense ultrashort laser pulse, the ultra-wide-band (from ultraviolet to x-ray) coherent high-order harmonic generation (HHG) can be carried out.^[1–18] HHG has been applied in the attosecond science^[19–21] and nonlinear optics in the XUV region.^[22]

The harmonic spectrum from atoms in the linearly polarized laser pulse presents typical characteristics: as the harmonic order increases, the intensity of the first few order harmonics drops rapidly, and then a so-called “plateau” appears, the harmonic intensity which changes little, and there is a cut-off (beyond this energy the harmonic intensity decreases rapidly) at the end of the plateau. The cut-off energy position satisfies the formula $E_c = I_p + 3.17U_p$, I_p is the ionization energy of the atom, and U_p is ponderomotive energy. The physical mechanism of HHG can be explained by a three-step model: the bound electron first tunnels through a potential barrier formed by the combined action of a laser electric field and atomic potential, then the ionized electron has the opportunity to return to the parent ion driven by the laser electric field, finally radiate high-energy photons.^[23,24]

Usually, linearly polarized driving fields have been con-

sidered to produce linearly polarized harmonics. The applications of the linearly polarized harmonic are limited in many aspects, such as x-ray magnetic circular dichroism,^[25] discrete molecular symmetry,^[26–30] spin dynamics,^[31–34] and recognizing chirality in molecules via photoelectron circular dichroism at their intrinsic timescales.^[35–37] Due to the larger frequency range of the harmonic spectrum, it is difficult to directly convert the harmonic polarization from the linear polarization to the circular one. Therefore, some schemes are proposed to generate the circularly polarized harmonic by shaping the driving pulse or controlling the atomic target. For generating circularly polarized harmonic, Yuan *et al.* adopted molecules interacting with the circularly polarized laser pulses with multiple frequencies.^[38] Kfir *et al.* found experimentally that the circularly polarized harmonic can be obtained from atoms irradiated by counter-rotating two-color (with frequencies of ω and 2ω) circularly polarized (CRTCCP) laser fields.^[39] This method was suggested firstly by Becker *et al.*,^[40,41] and investigated deeply in experiments and theories.^[25,39,42–45] When the atom is irradiated by the CRTCCP laser pulse, the polarization of the $3n + 1$ and $3n + 2$ order harmonics are the same as those of the fundamental and double frequencies, respectively. Furthermore, the $3n$ order harmonics in the HHG spectra are suppressed.^[39,46] The effect of the laser wavelength on the harmonic efficiency was discussed.^[47–50]

*Project supported by the National Key Research and Development Program of China (Grant Nos. 2019YFA0307700 and 2017YFA0403300), the National Natural Science Foundation of China (Grant Nos. 11627807, 11774175, 11534004, 11774129, 11975012, and 11604119), the Fundamental Research Funds for the Central Universities of China (Grant No. 30916011207), the Jilin Provincial Research Foundation for Basic Research, China (Grant No. 20170101153JC).

†Corresponding author. E-mail: yangyj@jlu.edu.cn

In order to achieve a higher HHG yield, a higher gas density is required. Due to the ionization of the atom irradiated by the driving laser pulse, the system is in the plasma state. The atomic potential is influenced by the ionized electron, and sometime the potential felt by the electron is described by the short-range Debye–Hückel model.^[51] The short-range potential model is also used to understand the role of the excited states on the generation of high harmonic. Faria *et al.* demonstrated the resonance effect of the potential function on atomic harmonics.^[52] Li *et al.* compared the harmonic and ionization characteristics of lithium atoms with short-range and long-range model potentials.^[53] Liu *et al.* analyzed the role of potential functions on the generation of attosecond pulses.^[54] In order to optimize the generation of high-order harmonic of an atom driven by a CRTCCP laser pulse, we investigate the potential function role on the process of HHG. The structure of the paper is as follows: In Section 2, the theoretical method of simulating the harmonic emission is introduced. In Section 3, the harmonic spectra from different potential functions in the CRTCCP laser pulse are presented, and the harmonic intensity changing with the driving laser intensity is analyzed. In Section 4 we summarize the results of this study. Atomic units are used throughout this paper unless stated otherwise.

2. Theory and models

Under the dipole approximation and the length gauge, the response of an atom irradiated by the strong laser field can be described by the time-dependent Schrödinger equation:

$$i\frac{\partial}{\partial t}\varphi(\mathbf{r},t) = \left[-\frac{1}{2}\nabla^2 + \mathbf{E}(t)\cdot\mathbf{r} + V(\mathbf{r}) \right] \varphi(\mathbf{r},t), \quad (1)$$

where $\varphi(\mathbf{r},t)$ is the time-dependent wave function, $V(\mathbf{r})$ is atomic potential, and $\mathbf{E}(t)$ is the electric field of the driving laser. In this paper, counter-rotating two-color circularly polarized laser fields are used:

$$\mathbf{E}_x(t) = \frac{1}{2}E_0f(t)[\cos(\omega t) + \cos(2\omega t)], \quad (2)$$

$$\mathbf{E}_y(t) = \frac{1}{2}E_0f(t)[\sin(\omega t) - \sin(2\omega t)], \quad (3)$$

where $f(t)$ is the envelope of the laser electric field (the trapezoidal envelope with 8 optical periods is adopted, and the rising and falling parts are one optical period, respectively), and $\omega = 0.057$ is the fundamental frequency of the laser pulse. The splitting operator method is used to solve the time-dependent Schrödinger Eq. (1). The wave function at instant $t_0 + \Delta t$ can be obtained from the wave function at instant t_0

$$\begin{aligned} & \varphi(\mathbf{r},t_0 + \Delta t) \\ &= \exp\left(\frac{-iU(\mathbf{r},t)\Delta t}{2}\right) \exp\left(-i\frac{\mathbf{p}^2}{2}\Delta t\right) \\ & \times \exp\left(\frac{-iU(\mathbf{r},t)\Delta t}{2}\right) \varphi(\mathbf{r},t_0) + O(\Delta t)^3, \quad (4) \end{aligned}$$

where $U(\mathbf{r},t) = \mathbf{E}(t)\cdot\mathbf{r} + V(\mathbf{r})$ and $\mathbf{p}^2/2$ are the potential energy and the kinetic energy of the system, respectively. By repeating the above evolution process, the space wave function $\varphi(\mathbf{r},t)$ at any instant can be calculated. The time-dependent dipole transition matrix element of the acceleration form at any instant can be produced from $\varphi(\mathbf{r},t)$ as

$$a_x(t) = \langle \varphi(\mathbf{r},t) \left| -\frac{\partial V(\mathbf{r})}{\partial x} - E_x(t) \right| \varphi(\mathbf{r},t) \rangle, \quad (5)$$

$$a_y(t) = \langle \varphi(\mathbf{r},t) \left| -\frac{\partial V(\mathbf{r})}{\partial y} - E_y(t) \right| \varphi(\mathbf{r},t) \rangle. \quad (6)$$

The corresponding harmonic radiation spectrum is obtained by

$$P_x(\omega) = \left| \frac{1}{\omega^2(t_{\text{fin}} - t_0)} \int_{t_0}^{t_{\text{fin}}} a_x(\omega) e^{-i\omega t} dt \right|^2, \quad (7)$$

$$P_y(\omega) = \left| \frac{1}{\omega^2(t_{\text{fin}} - t_0)} \int_{t_0}^{t_{\text{fin}}} a_y(\omega) e^{-i\omega t} dt \right|^2. \quad (8)$$

In order to understand the harmonic generation mechanism, the time-frequency behavior is calculated from the wavelet transform of the dipole moment

$$A_x(t_0, \omega) = \int_{t_i}^{t_{\text{fin}}} a_x(t) w_{t_0, \omega}(t) dt, \quad (9)$$

$$A_y(t_0, \omega) = \int_{t_i}^{t_{\text{fin}}} a_y(t) w_{t_0, \omega}(t) dt, \quad (10)$$

where $w_{t_0, \omega}(t) = \sqrt{\omega} W[\omega(t - t_0)]$ is the kernel of wavelet, and the Morlet wavelet is chosen as follows:

$$W(s) = \frac{1}{\sqrt{\tau}} e^{-is} e^{-\frac{s^2}{2\tau^2}}. \quad (11)$$

3. Results and discussion

The potential functions used in this paper are the long-range softened Coulomb potential $V(\mathbf{r}) = \frac{-1}{\sqrt{|\mathbf{r}|^2 + a_1}}$ and the short-range potential $V_s(\mathbf{r}) = \frac{(-1)e^{\beta|\mathbf{r}|}}{\sqrt{|\mathbf{r}|^2 + a_2}}$. Here $a_1 = 0.07$, $a_2 = 0.02$, $\beta = -0.3$ and atomic ground state energies are -0.9 (the ground state energy of the He atom) for two potentials. When atoms are irradiated by the CRTCCP laser pulse ($E_0 = 0.1015$), the corresponding HHG are shown in Figs. 1(a) and 1(b), respectively. The harmonic spectra generated from two model atoms have the same cut-off energy, and intensities of $3n$ harmonics are suppressed. There are some differences appeared in the spectra, for example, for the long-range model atom, $I_{20\text{th}} > I_{19\text{th}}$ (I represents the harmonic intensity). However, for the short-range model atom, the relative strengths of these two harmonics present opposite characteristics. Compared with the case of the long-range model atom, $I_{25\text{th}}$, $I_{26\text{th}}$, $I_{31\text{st}}$, and $I_{32\text{nd}}$ are suppressed for the short-range model atom. The above results demonstrate that the potential has an apparent affect on the harmonic spectra from the CRTCCP laser pulse.

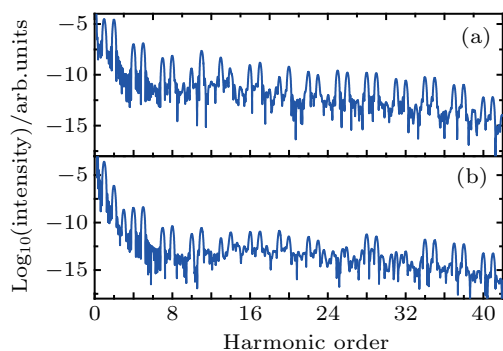


Fig. 1. Harmonic emission spectra of long-range (a) and short-range (b) atoms in the CRTCCP laser pulse.

In order to further understand the effect of the potential function on the harmonic intensity, we systematically investigate the intensity variation of the harmonic generated from the long-range model (Fig. 2(a)) and short-range model (Fig. 2(b)) atoms. To further clarify the harmonic feature, by using the strong-field approximation (SFA) scheme, figure 3 exhibits the HHG spectrum from the hydrogenic atom with the same ionization of the short-range one. It is found that the cut-off energies of the harmonic spectra of the atom increase with the increase of light intensity. For different models, one can clearly observe the emission of $3n + 1$ and $3n + 2$ order harmonics in the harmonic spectra.

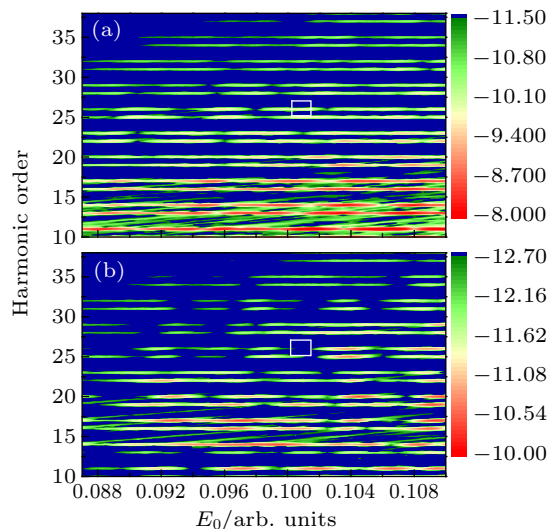


Fig. 2. The variation of harmonic spectra with the peak amplitude of the laser electric field calculated from the long-range model atom (a) and the short-range model atom (b).

The intuitive distinction of the harmonic spectra from the three cases is the non-integer order harmonic emission, as presented in Figs. 2 and 3. For the SFA calculation, one cannot observe the non-integer order harmonic emission in the photon spectra. For the harmonic generated from the short-range model atom, the non-integer order harmonic near the 15th harmonic can be found. While for the long-range model atom, we can see the non-integer order harmonics in the spectra range from 10th to 17th harmonic orders. The non-integer order harmonic emission can be attributed to the effect of the excited

state.^[55] Due to the existence of the excited state, under the action of the CRTCCP laser electric field, the electrons are more populated in the excited state. The electrons in the excited state have the opportunity to jump to the ground state to emit photons. The photon energy is no longer an integer multiple of the photon frequency, and the non-integer harmonic emission can be generated, as exhibited in Fig. 2. Although there is no excited state in the short-range atom, one can also observe the non-integer order harmonic emission. For a short-range model atom in the laser field, the light-induced dressed state^[56,57] appears. The transition between the laser-induced dressed state and the ground state contributes to the generation of the non-integer order harmonic of the short-range model atom. Compared to the long-range potential, the laser-induced dressed state induced in the short-range potential is at a higher energy level than the excited state of the long-range potential, so the non-integer order emission of the short-range potential appears in a higher energy range.

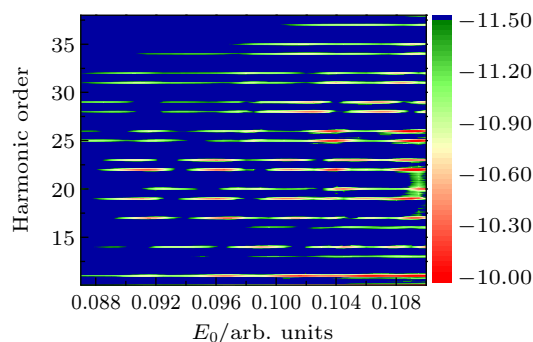


Fig. 3. The variation of harmonic spectra with the peak amplitude of the laser electric field calculated from the SFA.

The other difference among these calculations is the suppression of $3n + 1$ and $3n + 2$ order harmonics. For example, the 26th harmonic intensity from the short-range atom is obviously suppressed (white box in Fig. 2(b)) when $E_0 = 0.1015$ driven by the same CRTCCP laser pulse, the 26th harmonic intensity of long-range atom is higher (white box in Fig. 2(a)).

For understanding the physical mechanism of the suppression of $3n + 1$ and $3n + 2$ order harmonics, we study the transient process of harmonic quantum emission. The quantum trajectories of harmonic emission are obtained by wavelet transform. The path with the earlier ionization time and the later emission time is called the long trajectory, and the path with the later ionization time and the earlier emission time is called the short trajectory. The positive and negative slope branches in the red box in Fig. 4(a) correspond to the short and long quantum trajectories (the illustration shows two trajectories marked by the red box). Due to the different excitation states of the long-range and short-range Coulomb potentials, the ionization position and ionization time of the electrons in the two cases are different, the initial velocity of the electron ionization is also different, and the Coulomb potential tail

has an effect on the electrons moving after ionization, which will also lead to different electron trajectories of long-range and short-range Coulomb potential. Figure 4(a) presents the time-frequency analysis of the short-range model atom with the laser intensity $E_0 = 0.1015$. It can be seen from this figure that the harmonic emission almost occurs for every optical cycle. Thus we can qualitatively understand the supersession profile for $3n + 1$ and $3n + 2$ order harmonics from one optical cycle. Two typical quantum emission trajectories (circled by the red box in Fig. 4(a)) are selected. After selecting the main emission time area of a trajectory, the Fourier transform is performed on the dipole moment in this time period to obtain the information of the imaginary and real parts of the harmonic, which can be used to calculate the phase of the harmonic trajectory. According to the phase of the single trajectory, the phase difference between the two trajectories can be calculated.

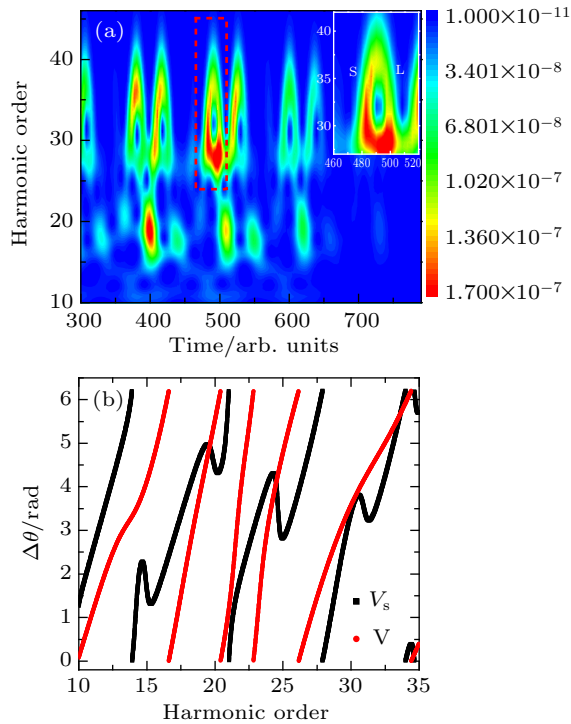


Fig. 4. (a) Wavelet analysis of the time-dependent dipole moment of the short-range model atom with laser intensity $E_0 = 0.1015$. (b) The variation of phase difference of two trajectories with harmonic orders for the harmonic from the long-range model atom (red circle) and short-range model atom (black square).

Figure 4(b) presents the variation of the phase difference with the harmonic order. For the 26th harmonic, the phase difference is about π for the short-range atom and 2π for the long-range atom, which means that the interference between the two quantum trajectories is destructive for the short-range atom and constructive for the long-range model atom. Thereby, in the harmonic spectrum from the short-range model atom, the suppression of the 26th order harmonic emission appears. The other suppressions of $3n + 1$ and $3n + 2$ order harmonics in Fig. 2 can also be understood by the similar analysis.

In the following, we systematically analyze the change of the HHG yield with the driving laser intensity. The harmonic yield can be defined as the energy integral in a fixed photon energy range.^[58] In this work, the harmonic yield is integrated from 31 eV to 62 eV: $\Delta Y = \int_{31 \text{ eV}}^{62 \text{ eV}} P(\omega) d\omega$. Figure 5 shows the change of the harmonic yield with the channel-closing number R ($R = (I_p + U_p)/\omega$) for the long-range model atom, the short-range atom and the SFA calculation. Here U_p is defined as $U_p = A_1^2/4 + A_2^2/4$, $A_1 = \frac{\sqrt{2}}{2} E_0/\omega$, $A_2 = \frac{\sqrt{2}}{2} E_0/2\omega$. With the increase of R , the HHG yield exhibits the oscillation profile in three cases. For the short-range atom and the SFA calculation, the peak of oscillation for the HHG yield appears near the integer R . There exists an offset for the peak position of the harmonic yield from the long-range model atom. The appearance of the oscillation can be explained by the channel closing effect.^[59] The ionization threshold is increased with the laser intensity due to the AC Stark effect. For the laser pulse with higher intensity, the electron needs to absorb more photons. When the R is an integer, an additional photon is required for the ionization. Thus the ionization is decreased with the increasing R (beyond an integer R). The reduction of the atomic ionization leads to the decrease of the harmonic yield. There are many excited states in the long-range model atom. Owing to the multi-photon resonance, the switch of the photon number may not occur at the position of the channel closing, but occur at the position corresponding to the intensity of the resonant laser between the ground state and the highly excited state.^[60]

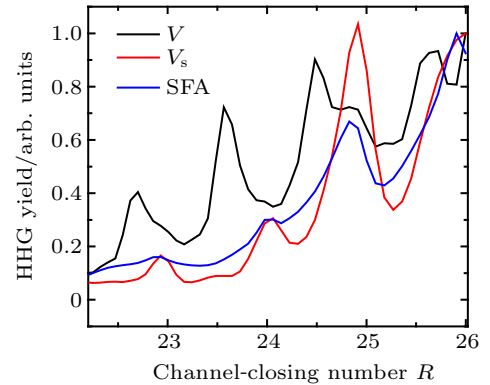


Fig. 5. Variation of the harmonic yield with R for calculations of the long-range model atom (black line), the short-range model atom (red line) and SFA (blue line), the laser intensity E_0 ranges from 0.0875 to 0.11.

From the above analysis, it is found that the harmonic intensity is affected by the potential function of the atom. In order to obtain a circularly polarized harmonic with high intensity, it is necessary to analyze the ellipticity of the harmonic emission. The ellipticity of the harmonic can be obtained by $\varepsilon = [(|D_+|) - (|D_-|)] / [(|D_+|) + (|D_-|)]$,^[61] where $D_{\pm} = \frac{1}{\sqrt{2}}(D_x \pm iD_y)$, D_x and D_y are x and y components of dipole accelerations in the frequency domain. Figure 6 presents the variation of the harmonic ellipticity with the peak

amplitude of the laser pulse. There are some harmonic ellipticity discrepancy between the long-range model and short-range model atoms, such as 25th harmonic (when $E_0 = 0.0925$ and $E_0 = 0.1015$), the ellipticity of long-range atom is close to 1 (circular polarization) and the ellipticity of short-range model atom is far off from 1 (elliptical polarization) (white box in Fig. 6). Combined with the calculation results in Figs. 2 and 6, for the long-range Coulomb potential, when the laser parameter E_0 is 0.096, the 25th harmonic with high-intensity circular polarization can be obtained. For the short-range Coulomb potential, when E_0 is 0.1035, the 26th harmonic with high intensity circular polarization can be generated. The polarization and intensity of different harmonics are closely related to the potential function, and the difference of the potential function is related to the plasma environment. Thus, it is possible to measure the state of the system by the analysis of the intensity and polarization of the harmonic.

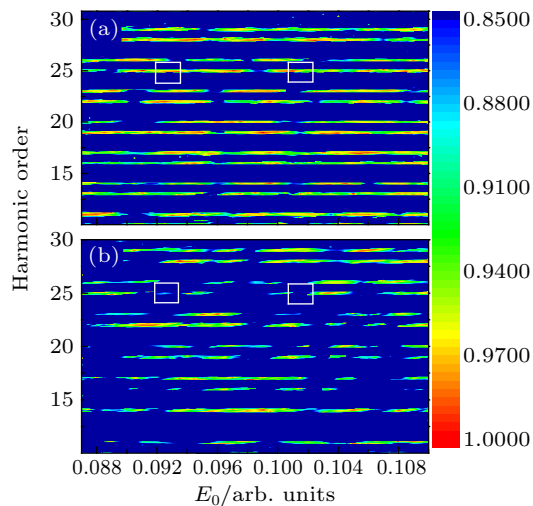


Fig. 6. The variation of the absolute value of ellipticity with the peak amplitude of the laser pulse calculated from the long-range (a) and short-range (b) model atoms.

4. Conclusions

In summary, we have theoretically studied the effect of the potential function on the harmonic emission of atoms driven by a bichromatic counter-rotating circularly polarized laser field. It is found that different potential functions result in an obvious distinction in the intensity minimum position of the harmonic spectra and the generation of the non-integer order harmonic emission. Through the analysis of quantum trajectories in one optical period, the intensity minimum in the harmonic spectra can attribute to the interference between different quantum trajectories. In addition, the variation of the harmonic ellipticity with the driving laser intensity is also discussed. Due to the sensitivity of the harmonic intensity and polarization on the potential function, one can generate the circularly polarized harmonic radiation with high intensity by optimizing atomic and molecular targets.

Acknowledgment

We acknowledge the High Performance Computing Center of Jilin University for supercomputer time and the high performance computing cluster Tiger@ IAMP.

References

- [1] Burnett, Reed K V and Knight P 1993 *J. Phys. B* **26** 561
- [2] Krause J L, Schafer K J and Kulander K C 1992 *Phys. Rev. Lett.* **68** 3535
- [3] Li X F, Huillier A L, Ferray M, Lompre L A and Mainfray G 1989 *Phys. Rev. A* **39** 5751
- [4] Han J X, Wang J, Qiao Y, Liu A H, Guo F M and Yang Y J 2019 *Opt. Express* **27** 8768
- [5] Paul P M, Tomas E S, Breger P, Mullot G, Aude F, Balcou P, Muller H G and Agostini P 2001 *Science* **292** 1689
- [6] Protopapas M, Keitel C H and Knight P L 1997 *Rep. Prog. Phys.* **60** 389
- [7] Schafer K J, Yang B, DiMauro L F and Kulander K C 1993 *Phys. Rev. Lett.* **70** 1599
- [8] Spielmann C, Burnett N H, Sartania S, Koppitsch R, Schnurer M, Kan C, Lenzner M, Wobrowschek P and Krausz F 1997 *Science* **278** 661
- [9] Song W J, Guo F M, Chen J G and Yang Y J 2018 *Acta Phys. Sin.* **67** 033201 (in Chinese)
- [10] Liu L, Zhao J, Yuan J M and Zhao Z X 2019 *Chin. Phys. B* **28** 114205
- [11] Pan Y, Guo F M and Yang Y J 2019 *Chin. Phys. B* **28** 113201
- [12] Xia C L, Lan Y Y, Li Q Q and Miao X Y 2019 *Chin. Phys. B* **28** 103203
- [13] Zhang J, Qi T, Pan X F, Guo J, Zhu K G and Liu X S 2019 *Chin. Phys. B* **28** 103204
- [14] Liu Y, Guo F M and Yang Y J 2019 *Acta Phys. Sin.* **68** 173202 (in Chinese)
- [15] Zhao Y T, Ma S Y, Jiang S C, Yang Y J, Zhao X and Chen J G 2019 *Opt. Express* **27** 34392
- [16] Pan Y, Guo F M, Yang Y J and Ding D J 2019 *Phys. Rev. A* **99** 033411
- [17] Zhao Y T, Ma S Y, Jiang S C, Zhao X, Chen J G and Yang Y J 2020 *Opt. Lett.* **45** 389787
- [18] Zhao Y T, Xu X Q, Jiang S C, Zhao X, Chen J G and Yang Y J 2020 *Phys. Rev. A* **101** 033413
- [19] Hentschel M, Kienberger R, Spielmann C, Reider G A, Milosevic N, Brabec T, Corkum P, Heinzmann U, Drescher M and Krausz F 2001 *Nature* **414** 509
- [20] Guo F M, Yang Y J, Jin M X, Ding D J and Zhu Q R 2009 *Chin. Phys. Lett.* **26** 053201
- [21] Xia C L and Miao X Y 2015 *Chin. Phys. Lett.* **32** 043202
- [22] Nabekawa Y, Hasegawa H, Takahashi E J and Midorikawa K 2005 *Phys. Rev. Lett.* **94** 043001
- [23] Corkum P B 1993 *Phys. Rev. Lett.* **71** 1994
- [24] de Morisson Faria C F, Dorr M and Sandner W 1998 *Phys. Rev. A* **58** 2990
- [25] Kfir O, Grychtol P and Turgut E 2015 *Nat. Photon.* **9** 99
- [26] Reich D M and Madsen L B 2016 *Phys. Rev. Lett.* **117** 133902
- [27] Baykusheva D, Ahsan M S, Lin N and Jakob H 2016 *Phys. Rev. Lett.* **116** 123001
- [28] Neufeld O, Ayuso D, Decleva P, Ivanov M, Smirnova O and Cohen O 2019 *Phys. Rev. X* **9** 031002
- [29] Neufeld O, Ayuso D, Decleva P, Ivanov M, Smirnova O and Cohen O 2019 *Nonlinear Optics (NLO) OSA Technical Digest (Optical Society of America, 2019) paper NM1A.2*
- [30] Miao X Y and Du H N 2013 *Phys. Rev. A* **87** 053403
- [31] Miao X Y and Zhang C P 2014 *Phys. Rev. A* **89** 033410
- [32] Graves C, Reid A and Wang T 2013 *Nat. Mater.* **12** 293
- [33] Eisebitt S, Luning J, Schlott W F, Lorgen M, Hellwing O, Eberhardt W and Stohr J 2004 *Nature* **432** 885
- [34] Radu I, Vahaplar K and Stamm C 2011 *Nature* **472** 205
- [35] Boeglin C, Beaupaire E, Halte V, Lopez-Flores V, Stamm C, Pontius N, Durr H A and Bigot J Y 2010 *Nature* **465** 458
- [36] Cireasa R, Boguslavskiy A and Pons B 2015 *Nat. Phys.* **11** 654
- [37] Travnikova O, Liu J C, Lindblad A, Nicolas C, Söderström J, Kimberg V, Gelmukhanov F and Miron C 2010 *Phys. Rev. Lett.* **105** 233001
- [38] Ferré A, Handschin C, Dumergue M *et al.* 2015 *Nat. Photon.* **9** 93

- [38] Yuan K J and Bandrauk A D 2019 *Phys. Rev. A* **100** 033420
- [39] Fleischer A, Kfir O, Diskin T, Sidorenko P and Cohen O 2014 *Nat. Photon.* **8** 543
- [40] Eichmann H, Egbert A, Nolte S, Momma C, Wellegehausen B, Becker W, Long S and McIveret J K 1995 *Phys. Rev. A* **51** R3414
- [41] Milošević D B and Becker W 2000 *Phys. Rev. A* **62** 011403
- [42] Milošević D B, Becker W and Kopold R 2000 *Phys. Rev. A* **61** 063403
- [43] Fan T, Grychtol P and Kunt R 2015 *Proc. Natl. Acad. Sci. USA* **112** 14206
- [44] Jiménez-Galán Á, Zhavoronkov N, Schloz M, Morales F, Ivanov M *et al.* 2017 *Opt. Express* **25** 22880
- [45] Dorney K M, Ellis J L, Carlos H G, Hickstein D D, Mancuso C A, Nathan B, Fan T, Fan G Y, Zusin D, Gentry C, Grychtol P, Kapteyn H C and Murnane M M 2017 *Phys. Rev. Lett.* **119** 063201
- [46] Milošević D B 2015 *J. Phys. B* **48** 171001
- [47] Tate J, Auguste T, Muller H G, Salières P, Agostini P and DiMauro L F 2007 *Phys. Rev. Lett.* **98** 013901
- [48] Frolov M V, Manakov N L and Starace A F 2008 *Phys. Rev. Lett.* **100** 173001
- [49] Colosimo P, Doumy G, Blaga I, Wheeler J, Hauri C, Catoire F, Tate J, Chirla R, March A M, Paulus G G, Muller H G, Agostini P and DiMauro L F 2008 *Nat. Phys.* **4** 386
- [50] Milošević D B, Hasovic E, Odzak S and Becker W 2008 *J. Mod. Optic* **55** 2653
- [51] Harris G M 1962 *Phys. Rev.* **125** 1131
- [52] de Morisson Faria C F, Kopold R, Becker W and Rost J M 2002 *Phys. Rev. A* **65** 023404
- [53] Li P C, Zhou X X, Dong C Z and Zhao S F 2004 *Acta Phys. Sin.* **53** 750 (in Chinese)
- [54] Liu Y, Cheng J, Guo F M and Yang Y J 2016 *Acta Phys. Sin.* **65** 033201 (in Chinese)
- [55] Yan Y, Guo F M, Wang J, Chen J G and Yang Y J 2018 *Chin. Phys. B* **27** 083202
- [56] Fearnside A S, Potvliege R M and Shakeshaft R 1995 *Phys. Rev. A* **51** 1471
- [57] Chen S, Bell M J, Beck A R, Mashiko H, Wu M, Pfeiffer A N, Gaarde M B, Neumark D M, Leone S R and Schafer K J 2012 *Phys. Rev. A* **86** 063408
- [58] Jackson J D 1998 *Classical Electrodynamics*
- [59] Ishikawa K L, Schiessl K, Persson E and Burgdörfer J 2009 *Phys. Rev. A* **79** 033411
- [60] Muller H G 1999 *Phys. Rev. A* **60** 1341
- [61] Odzak S and Milošević D B 2015 *Phys. Rev. A* **92** 053416